

Reduction of the Ferrous α -Verdoheme–Cytochrome b_5 ComplexChristopher O. Damaso,[†] Nick D. Rubie,[‡] Pierre Moënne-Loccoz,[‡] and Mario Rivera^{*†}*Department of Chemistry, University of Kansas, Lawrence, Kansas 66045-7582, and Department of Environmental & Biomolecular Systems, OGI School of Science & Engineering, Oregon Health & Science University, Beaverton, Oregon 97006-8921*

Received July 20, 2004

The ferrous α -verdoheme–cytochrome b_5 complex, $[\text{Fe}^{\text{II}}(\text{verdoheme})]^+$, has been prepared and characterized spectroscopically. Anaerobic addition of excess sodium dithionite to $[\text{Fe}^{\text{II}}(\text{verdoheme})]^+$ at pH 10 produces a one-electron-reduced species with spectroscopic characteristics that suggest a ferrous hexacoordinated verdoheme π neutral radical best formulated as a $[\text{Fe}^{\text{II}}(\text{verdoheme}\bullet)] \rightarrow [\text{Fe}^{\text{I}}(\text{verdoheme})]$ resonance hybrid. At lower pH values (7.0 and 8.0) the one-electron-reduced species is shown to disproportionate to produce the resting state $[\text{Fe}^{\text{II}}(\text{verdoheme})]^+$ complex and the two-electron-reduced $[\text{Fe}^{\text{II}}(\text{verdoheme})]^-$ anion. The latter might also be formulated as a resonance hybrid $[\text{Fe}^{\text{I}}(\text{verdoheme}\bullet)]^- \rightarrow [\text{Fe}^{\text{II}}(\text{verdoheme})]^-$. The disproportionation reaction becomes very slow as the pH is raised above 9.0. Exposure of the one-electron- or two-electron-reduced verdoheme complexes of cytochrome b_5 to O_2 results in rapid and quantitative reoxidation to the resting state $[\text{Fe}^{\text{II}}(\text{verdoheme})]^+$ complex.

Introduction

The catalytic degradation of heme is an important physiological process that in mammals is carried out by the enzyme heme oxygenase (HO). In this process (Scheme 1)^{1,2} hemin bound to HO accepts one electron to form the iron(II) heme–HO complex, which binds O_2 to form an oxyferrous complex. The latter accepts a second electron and is thereby transformed into a ferric hydroperoxide species, which hydroxylates the α -meso carbon to form α -meso-hydroxyheme. The α -meso-hydroxyheme intermediate is converted to α -verdoheme³ via an O_2 -dependent elimination of the α -meso carbon as CO and concomitant incorporation of an oxygen atom at this position. Consequently, α -verdoheme is a protoheme IX possessing an oxygen atom in place of the α -meso carbon. In the last step of heme oxidation α -verdoheme is converted to biliverdin in an electron- and oxygen-dependent manner. The chemistry of verdoheme has received relatively little attention despite the fact that it is

an important intermediate in the process of heme degradation. The most recent and definitive work on verdoheme chemistry comes from the model verdoheme studies of Balch and co-workers. For instance, these investigators determined the X-ray crystal structure of octaethylverdoheme,^{4,5} thus establishing conclusively the structure of verdoheme and resolving a longstanding controversy regarding the structure of the macrocycle. These investigators also demonstrated with model complexes that the iron center in verdoheme can undergo a set of reactions that include changes in oxidation state, axial coordination state, and spin state, while maintaining the structural integrity of the macrocycle.^{4,6}

Two pathways have been proposed for the oxidation of verdoheme to biliverdin:^{1,7} (a) One path implicates the formation of a ferrous verdoheme– O_2 complex (reaction 1 in Scheme 2), followed by the addition of one electron to the ferrous–oxy complex to form a ferric peroxide intermediate. The latter is assumed to attack the verdoheme macrocycle to form Fe^{III} –biliverdin. (b) A different path assumes the one-electron reduction of ferrous verdoheme

* To whom correspondence should be addressed. E-mail: mrivera@ku.edu.
[†] University of Kansas.

[‡] Oregon Health & Science University.

- (1) Ortiz de Montellano, P. R.; Auclair, K. In *The Porphyrin Handbook, 12, Heme Oxygenase Structure and Function*; Kadish, K. M., Smith, K. M., Guillard, R., Eds.; Elsevier: New York, 2003; pp 183–210.
- (2) Ortiz de Montellano, P. R.; Wilks, A. *Adv. Inorg. Chem.* **2000**, *51*, 359–407.
- (3) Yoshida, T.; Noguchi, M.; Kikuchi, G. *J. Biochem.* **1980**, *88*, 557–563.

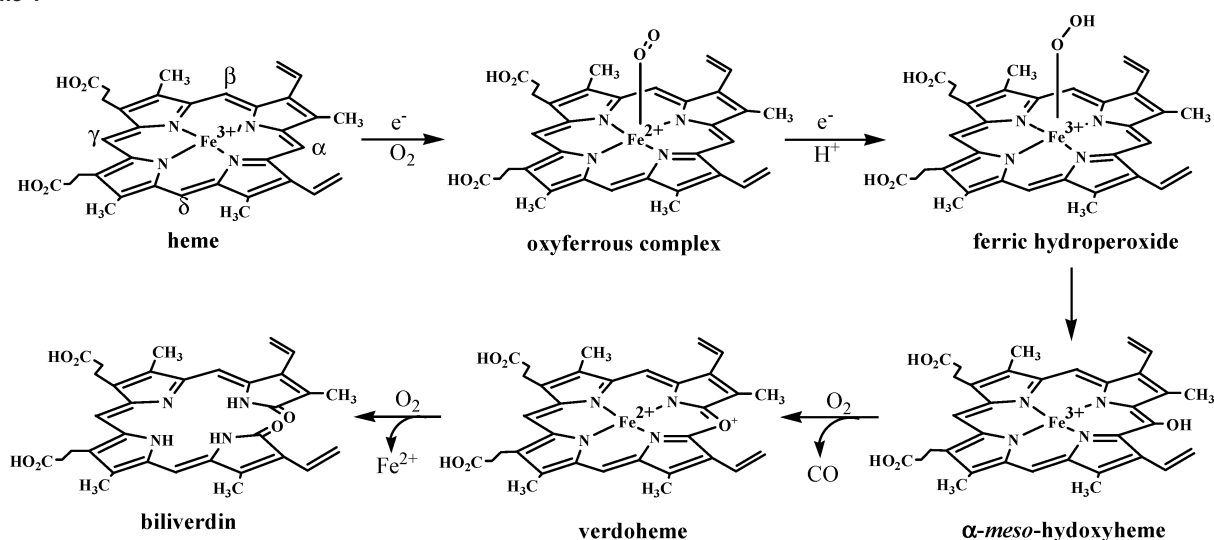
(4) Balch, A. L.; Noll, B. C.; Safari, N. *Inorg. Chem.* **1993**, *32*, 2901–2905.

(5) Balch, A. L.; Koerner, R.; Olmstead, M. M. *J. Chem. Soc., Chem. Commun.* **1995**, 873–874.

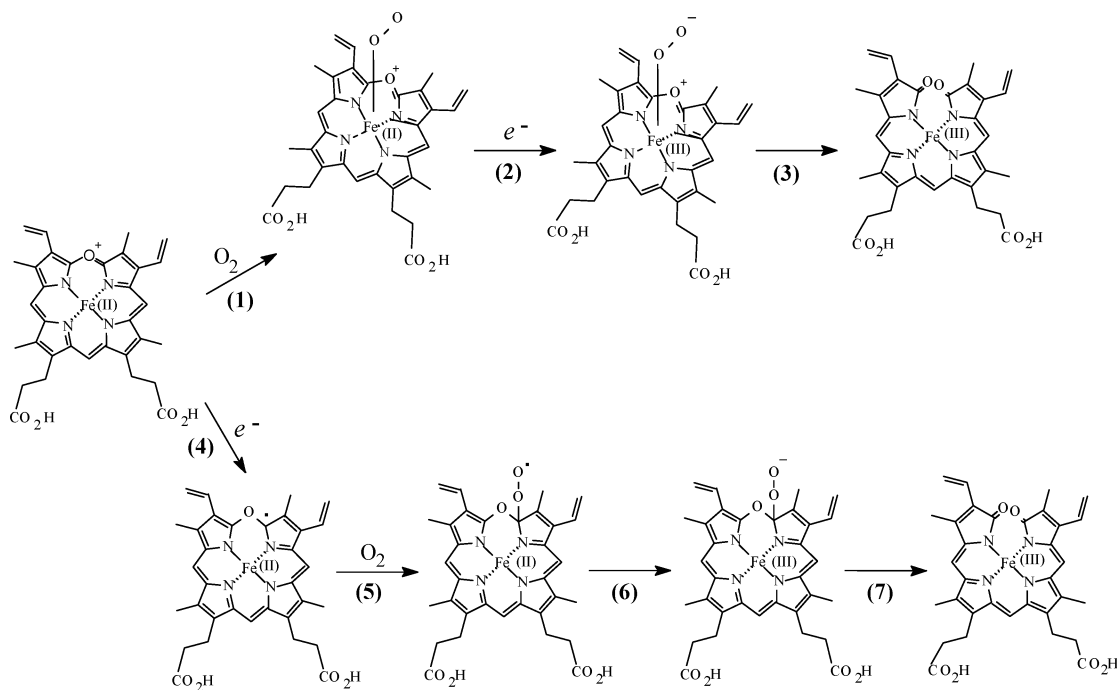
(6) Balch, A. L.; Latos-Grazynski, L.; Noll, B. C.; Olmstead, M. M.; Sztrenberg, L.; Safari, N. *J. Am. Chem. Soc.* **1993**, *115*, 1422–1429.

(7) Sano, S.; Sano, T.; Morishima, I.; Shiro, Y.; Maeda, Y. *Proc. Natl. Acad. Sci. U.S.A.* **1986**, *83*, 531–535.

Scheme 1



Scheme 2



(reaction 4 in Scheme 2); the latter reacts with O_2 to form an isoporphyrin-type intermediate, which can be converted into a peroxide bound intermediate that decays to Fe^{III} –biliverdin. Efforts to obtain evidence for the formation of an Fe^{II} –verdoheme– O_2 complex (reaction 1 in Scheme 2) in heme oxygenase have been stymied by the very high reactivity of verdoheme toward O_2 .⁸ Consequently, it has not been possible to conclusively prove that the activation of O_2 at Fe^{II} –verdoheme occurs in a manner akin to that by which O_2 is activated at heme centers, namely, via the initial formation of an O_2 adduct, followed by its reduction to coordinated peroxide.^{1,2} Regarding the alternative path (reaction 4 in Scheme 2), it has been reported that Fe^{II} –verdoheme or Zn^{II} –verdoheme complexes of myoglobin are degraded to a species presumed to be biliverdin when treated with ascorbate in the presence of O_2 . These findings were interpreted to suggest that the iron in verdoheme is not necessary for its oxidation to biliverdin and that the mechanism of oxidation likely proceeds via the reduction of the verdoheme macrocycle,⁹ as is shown by reaction 4 in Scheme 2.

heme or Zn^{II} –verdoheme complexes of myoglobin are degraded to a species presumed to be biliverdin when treated with ascorbate in the presence of O_2 . These findings were interpreted to suggest that the iron in verdoheme is not necessary for its oxidation to biliverdin and that the mechanism of oxidation likely proceeds via the reduction of the verdoheme macrocycle,⁹ as is shown by reaction 4 in Scheme 2.

In the same context, it has also been reported that the bis-(pyridine) complex of verdoheme can be reduced to an Fe^{II} –verdoheme π -neutral radical. When the latter was exposed to O_2 , the electronic absorption spectrum of the π -neutral radical changed to a spectrum displaying a broad peak centered at 778 nm. This spectrum was assumed to originate

(8) Migita, C. T.; Matera, K. M.; Ikeda-Saito, M.; Olson, J. S.; Fujii, H.; Yoshimura, T.; Zhou, H.; Yoshida, T. *J. Biol. Chem.* **1998**, *273*, 945–949.

(9) Modi, S. J. *Inorg. Biochem.* **1993**, *52*, 297–304.

from biliverdin, although the formation of biliverdin was not established rigorously.^{10,11} Taken together, these observations suggest that one possible path for the oxidation of verdoheme involves reduction of the macrocycle. To study the feasibility of verdoheme ring reduction in a protein environment and to further probe the possibility of oxidizing verdoheme to biliverdin in a path that does not involve the participation of the verdoheme iron, we reconstituted cytochrome *b*₅ with verdoheme. Herein we report our initial investigations aimed at probing the chemical properties of verdoheme in a protein environment where the verdoheme iron is coordinatively saturated.

Experimental Section

Synthesis and Purification of α -Verdohemochrome. A mixture of verdohemochrome isomers was prepared by the coupled oxidation reaction utilizing previously published methods.^{6,12} Separation of verdoheme isomers was accomplished by reverse-phase HPLC according to previously described methodology.¹³ HPLC was performed with a Dynamax model HPXL solvent delivery system equipped with a Dynamax absorbance detector model UV-D II (Rainin Instrument Co. Inc., Woburn, MA). The elution profile was monitored at 398 nm, and the separation was performed on a Vydac C18 column (10 × 250 mm) from GraceVydac (Hesperia, CA). Separation of all four verdoheme isomers was attained under the following conditions: 25 °C; flow rate = 5 mL/min; a 60-min concave gradient starting at 15% solution B and ending at 60% solution B. Solution A is water–pyridine (90:10 v/v) adjusted to pH 7.0 with trifluoroacetic acid, and solution B is acetonitrile. The four verdoheme regioisomers eluted in the order α (33 min), β (36 min), γ (43 min), and δ (39 min). The fraction containing α -verdoheme was collected and transferred to a rotary evaporator to eliminate acetonitrile from the mixture, leaving behind α -verdoheme dissolved in a mixture of water and ~10% (v/v) pyridine. This solution was subsequently used to reconstitute apo-OM *b*₅.

Preparation of the α -Verdoheme Cytochrome *b*₅ Complex. Rat liver outer mitochondrial membrane cytochrome *b*₅ (OM *b*₅) was expressed in *Escherichia coli* cells BL21(DE3) previously transformed with a pET 11a plasmid harboring a synthetic gene coding for OM *b*₅.¹⁴ Purification of the protein to homogeneity was accomplished by following previously established methods.^{15,16} The heme was extracted according to previously reported methodology¹⁷ with a few minor variations: Ice-cold OM *b*₅ (0.03 mM) dissolved in 30 mL phosphate buffer ($\mu = 0.1$, pH 7) was titrated with 0.1 M HCl to adjust the pH to ~1, and the heme was extracted with an equal volume of ice-cold butanone. Quantitative removal of heme from OM *b*₅ was accomplished by three successive extractions with ice-cold butanone. If the pH is adjusted to a value of 2.0, which is the pH value typically utilized to extract heme from

other proteins, removal of heme from OM *b*₅ is not complete. Apo-OM *b*₅ in the resultant aqueous layer was refolded at 4 °C by dialyzing it against a buffer containing 0.6 mM sodium bicarbonate and 1 mM EDTA at pH 10.3. This step was followed by further dialysis against phosphate buffer ($\mu = 0.1$, pH 7.0) and subsequent concentration of the apoprotein to a volume of approximately 10 mL.

The solution containing apoprotein (~1 μ mol) was mixed with the solution containing α -verdoheme (10% excess) and the resultant mixture stirred slowly for ~20 h at room temperature. The progress of the reconstitution reaction was monitored by electronic absorption spectroscopy; complete reconstitution is indicated by a spectrum exhibiting bands at 400 nm (Soret) and at 700 nm. The α -verdoheme–OM *b*₅ complex was dialyzed against phosphate buffer ($\mu = 0.1$, pH 7) at room temperature to remove the excess pyridine and then concentrated with the aid of a Centriprep centrifugal filter (Millipore Corp., Bedford, MA) to a final volume of 3 mL. The concentrated α -verdoheme–OM *b*₅ solution was loaded onto a Sephadex G-10 column (2.5 cm × 20 cm) for further purification and eluted with phosphate buffer, $\mu = 0.1$ and pH 7.0.

Electronic Absorption Spectroscopy. Reduction of the ferrous α -verdoheme–OM *b*₅ complex was conducted under inert atmosphere at 25 °C in a modified quartz cuvette connected to a Schlenk line. A 4.5 mL solution containing ferrous α -verdoheme–OM *b*₅ complex in phosphate buffer (~7 μ M) was degassed for at least 1 h by bubbling argon through a polyethylene capillary tube (0.8 mm i.d.) inserted via a small port in the anaerobic cell. The port was capped with a rubber septum after removing the capillary tube, and the cell was maintained under slight positive pressure of argon with the aid of the Schlenk line. The anaerobic solution of the ferrous α -verdoheme *b*₅ complex was then treated with an air-free solution of sodium dithionite (~5–10 equiv), which was introduced through the rubber septum using a gastight syringe. Electronic absorption spectra were collected at appropriate intervals with the aid of a UV–vis S2000 spectrophotometer (Ocean Optics, Dunedin, FL).

Resonance Raman Spectroscopy. Typical enzyme concentrations for the resonance Raman (RR) experiments were between 30 and 100 μ M in either pH 7 potassium phosphate or pH 10 CAPS (3-[cyclohexylamino]-1-propanesulfonic acid) buffer. Samples were handled in an anaerobic chamber (omni-lab system, Vacuum Atmospheres, Hawthorne, CA), and reduction of the ferrous α -verdoheme *b*₅ complex was performed by adding 5 to 6 equiv of sodium dithionite. Electronic absorption spectra were collected directly in the Raman capillaries at room temperature using a Varian Cary 50 spectrophotometer. Resonance Raman spectra were collected on a McPherson 2061/207 spectrograph in a 0.67 m (McPherson, Chelmsford, MA) configuration equipped with a Kaiser Optical supernotch filter to attenuate Rayleigh scattering. Raman scattered light was dispersed using either an 1800 or 2400 gr/mm holographic grating and detected by a liquid-nitrogen-cooled Princeton Instruments LN-1100PB CCD detector (Roper Scientific, Trenton, NJ). A Coherent Innova 302 krypton ion laser (413 nm) and a Coherent Innova 90 argon ion laser (458 nm) (Coherent, Santa Clara, CA) were used as excitation sources. Laser power was maintained below 10 mW at the sample to prevent potential degradation of the samples. Electronic absorption spectra were acquired before and after RR data collection to ensure sample integrity. Vibrational frequencies were calibrated relative to an indene standard and are accurate to ± 1 cm⁻¹.

Electron Paramagnetic Resonance Spectroscopy. EPR spectra were collected using an E500 X-band EPR spectrometer equipped

- (10) Tajima, K.; Tada, K.; Yasui, A.; Ohya-Nishiguchi, H.; Kazuhiko, I. *J. Chem. Soc., Chem. Commun.* **1993**, 282–284.
- (11) Tajima, K.; Shimizu, K.; Mano, H.; Mukai, M.; Azuma, N. *J. Chem. Soc., Chem. Commun.* **1995**, 601–603.
- (12) Saito, S.; Itano, H. A. *Proc. Natl. Acad. Sci. U.S.A.* **1982**, *79*, 1393–1397.
- (13) Sakamoto, H.; Omata, Y.; Adachi, Y.; Palmer, G.; Noguchi, M. *J. Inorg. Biochem.* **2000**, *82*, 113–121.
- (14) Rivera, M.; Barillas-Mury, C.; Christensen, K. A.; Little, J. W.; Wells, M. A.; Walker, F. A. *Biochemistry* **1992**, *31*, 12233–12240.
- (15) Altuve, A.; Silchenko, S.; Lee, K. H.; Kuczera, K.; Terzyan, S.; Zhang, X.; Benson, D. R.; Rivera, M. *Biochemistry* **2001**, *40*, 9469–9483.
- (16) Altuve, A.; Wang, L.; Benson, D. R.; Rivera, M. *Biochem. Biophys. Res. Commun.* **2004**, *305*, 840–845.
- (17) Teale, F. W. J. *Biochim. Biophys. Acta* **1959**, *35*, 543.

Reduction of Ferrous α -Verdoheme–Cytochrome b_5

with a superX microwave bridge (Bruker Biospin, Billerica, MA). A superhigh Q cavity was used for samples at 77 K and room temperature.

Results

Preparation and Spectroscopic Characterization of the α -Verdoheme– b_5 Complex. Addition of a solution of apocytochrome b_5 to a solution of α -verdohemochrome in aqueous pyridine, followed by elimination of excess pyridine by dialysis and subsequent purification in a Sephadex G10 column, yields a homogeneous solution of the α -verdoheme–OM b_5 complex (hereafter abbreviated $[\text{Fe}^{\text{II}}(\text{verdoheme}-b_5)]^+$). Remarkably, the verdoheme– b_5 complex is stable to air, so the reconstitution reaction was not carried out under anaerobic conditions. In contrast, reconstitution of heme oxygenase with verdoheme results in the formation of a highly O_2 -sensitive complex.^{18–21} The electronic absorption spectrum of $[\text{Fe}^{\text{II}}(\text{verdoheme}-b_5)]^+$ (Figure 1A) is very similar to that of the pyridine α -verdohemochrome (Figure 1B), differing only in that the Soret and visible bands of the former are slightly red shifted. The electronic absorption spectrum of $[\text{Fe}^{\text{II}}(\text{verdoheme}-b_5)]^+$ indicates that the oxidation state of the iron remains as Fe(II), despite the fact that reconstitution and purification of the apo cytochrome b_5 complex was carried out in air over a period of ~ 48 h. Additional evidence in favor of a ferrous oxidation state stems from the fact that the complex is EPR silent. The resonance Raman (RR) spectrum of the $[\text{Fe}^{\text{II}}(\text{verdoheme}-b_5)]^+$ complex obtained with 413-nm excitation is dominated by a strong and sharp band at 1609 cm^{-1} and medium bands at 1250 , 1362 , 1443 , 1485 , and 1573 cm^{-1} (Figure 2). These spectral features are nearly identical to those observed by Takahashi and co-workers with bis(imidazole)ferrous protoverdoheme IX α , but they are also similar to those exhibited by the $[\text{Fe}^{\text{II}}(\text{verdoheme}-\text{myoglobin})]^+$ complex and the corresponding cyanocomplex $[(\text{CN}^-)\text{Fe}^{\text{II}}(\text{verdoheme}-\text{myoglobin})]$.²⁰ These observations are consistent with coordination of the verdoheme iron by His-39 and His-63 in OM b_5 . However, compared to heme skeletal modes, those displayed by the verdoheme macrocycle are less sensitive to the coordination state of the central iron. The similarity of the RR data obtained from the verdoheme complexes of myoglobin, heme oxygenase, and cytochrome b_5 indicate that the influence of the protein matrix on the macrocycle is comparable in all three proteins. Hence, the stability of the $[\text{Fe}^{\text{II}}(\text{verdoheme}-b_5)]^+$ complex to air is likely a consequence of hexacoordinated iron(II) verdoheme.^{7,12,22}

Reduction of the Ferrous α -Verdoheme– b_5 Complex.

It is well established that electron-withdrawing substituents

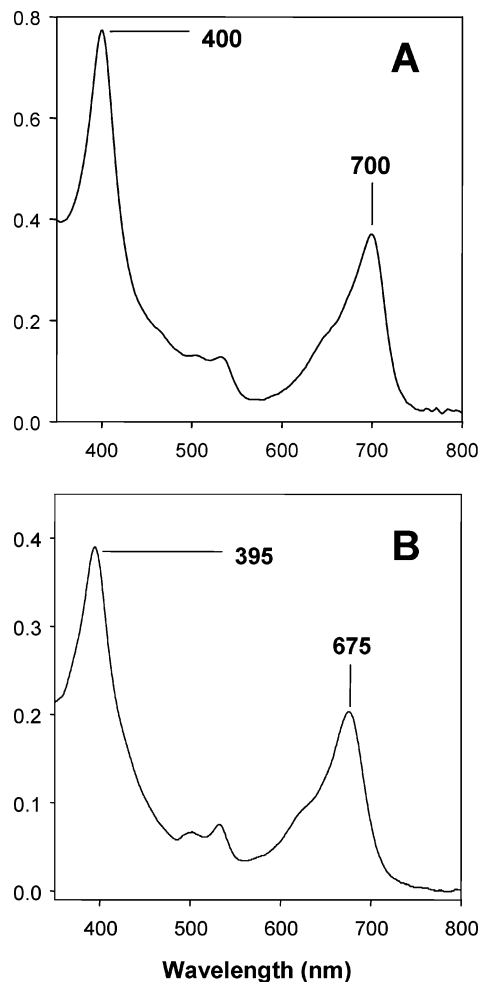


Figure 1. Electronic absorption spectra of (A) α -verdoheme– b_5 complex, $[\text{Fe}^{\text{II}}(\text{verdoheme})]^+$, and (B) pyridine α -verdohemochrome.

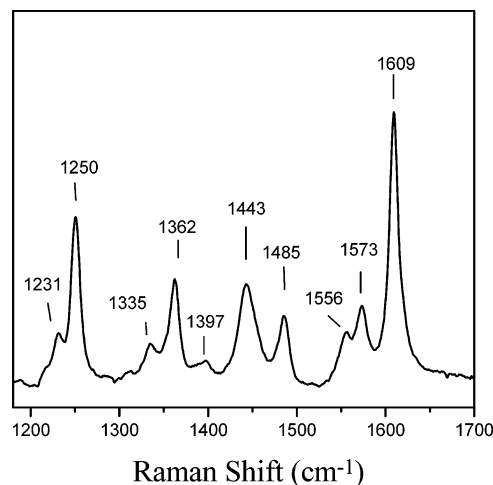


Figure 2. Resonance Raman spectrum of $[\text{Fe}^{\text{II}}(\text{verdoheme})]^+$ collected using 413 nm excitation.

on metalloporphyrins induce significant positive shifts in the reduction potential of these complexes relative to those exhibited by unsubstituted porphyrins.²³ It has therefore been possible to generate iron porphyrins with formal oxidation states of Fe^{I} and Fe^{0} using porphyrins bearing cyanide groups

(23) Kadish, K. M.; Boisselier-Cocolios, B.; Simonet, B.; Chang, D.; Ledon, H.; Cocolios, P. *Inorg. Chem.* **1985**, *24*, 2148–2156.

- (18) Sakamoto, H.; Omata, Y.; Hayashi, S.; Harada, S.; Palmer, G.; Noguchi, M. *Eur. J. Biochem.* **2002**, *269*, 5231–5239.
- (19) Zhang, X.; Fujii, H.; Mansfield Matera, K.; Taiko Migita, C.; Sun, D.; Sato, M.; Ikeda-Saito, M.; Yoshida, T. *Biochemistry* **2003**, *42*, 7418–7426.
- (20) Takahashi, S.; Matera, K. M.; Fujii, H.; Zhou, H.; Ishikawa, K.; Yoshida, T.; Ikeda-Saito, M.; Rousseau, D. L. *Biochemistry* **1997**, *36*, 1402–1410.
- (21) Liu, Y.; Moëne-Loccoz, P.; Loehr, T. M.; Ortiz de Montellano, P. R. *J. Biol. Chem.* **1997**, *272*, 6909–6917.
- (22) Rodriguez, J. C.; Desilva, T.; Rivera, M. *Chem. Lett.* **1998**, 353–354.

on their β -pyrrole carbons, i.e., tetracyanotetraphenyl porphyrin, $(\text{CN})_4\text{TPP}$.^{23–27} Similarly, the electronegative oxygen atom contained within the ring of verdoheme is expected to facilitate reduction of the $[\text{Fe}^{\text{II}}(\text{verdoheme}-b_5)]^+$ complex. Indeed, addition of dithionite to an anaerobic solution of $[\text{Fe}^{\text{II}}(\text{verdoheme}-b_5)]^+$ results in significant changes in the electronic absorption spectrum that are consistent with reduction (vide infra). Moreover, the type of compound obtained upon treatment of $[\text{Fe}^{\text{II}}(\text{verdoheme}-b_5)]^+$ with dithionite depends on the pH of the solution. We will first describe these changes at pH 10 and then discuss the studies performed at pH values between 7.0 and 10.0.

(a) Reduction of Fe^{II} α -Verdoheme- b_5 at pH 10.0.

When dithionite is added to a solution of $[\text{Fe}^{\text{II}}(\text{verdoheme}-b_5)]^+$ at pH 10 under anaerobic conditions the Soret band (400 nm) and the visible band (700 nm) corresponding to the spectrum of $[\text{Fe}^{\text{II}}(\text{verdoheme}-b_5)]^+$ decrease, with a concomitant increase of bands at 446 and 757 nm (Figure 3A). These changes occur with clear isosbestic points at 415 and 722 nm. The resultant spectrum is similar to that reported for the π -neutral radical of Zn^{II} - and Fe^{II} -verdoheme dimethyl ester complexes obtained electrochemically in DMF-pyridine (6:4) solutions^{10,11} and therefore suggests the formation of an α -verdoheme- b_5 π -neutral radical complex at pH 10.0. The EPR spectrum of this species at 90 K is rhombic with g values of 2.02, 2.00, and 1.925 (Figure 3B). At room temperature, the EPR spectrum is composed of an isotropic signal at $g = 2.005$ and retains a substantial rhombic signal with g values of 2.066, 2.005, and 1.929 (Figure 3C). These spectra suggest some degree of delocalization of unpaired electron density between the metal center and the verdoheme orbitals and therefore a reduced α -verdoheme-OM b_5 complex at pH 10 that may be formulated as a resonance hybrid of $[\text{Fe}^{\text{I}}(\text{verdoheme}-b_5)]$ and $[\text{Fe}^{\text{II}}(\text{verdoheme}-b_5\bullet)]$. For simplicity this complex will be referred to as $[\text{Fe}^{\text{II}}(\text{verdoheme}\bullet)]$. It is noteworthy that a similar delocalization of charge in iron porphyrins has led to the formulation of resonance hybrids Fe^{I} anion, $[\text{Fe}^{\text{I}}(\text{CN})_4\text{TPP}]^-$, and an Fe^{II} radical anion, $[\text{Fe}^{\text{II}}(\text{CN})_4\text{TPP}\bullet]^-$.^{23–25,27} The presence of both an isotropic and a broad anisotropic signal in the EPR spectrum obtained at ambient temperature suggests the presence of two populations, one with a pure macrocycle radical, which gives rise to the isotropic signal, and a second population perhaps best characterized as a resonance hybrid between $[\text{Fe}^{\text{I}}(\text{verdoheme})]$ and $[\text{Fe}^{\text{II}}(\text{verdoheme}\bullet)]$, which gives rise to the anisotropic signal. The reasons for the presence of two populations are not clear at present. Nevertheless, it is interesting that the anisotropic signal, which is affected by spin density residing in the iron d orbitals is observable at room temperature. This suggests that the rate of relaxation of the unpaired electron is simultaneously influenced by the relaxation properties of spin

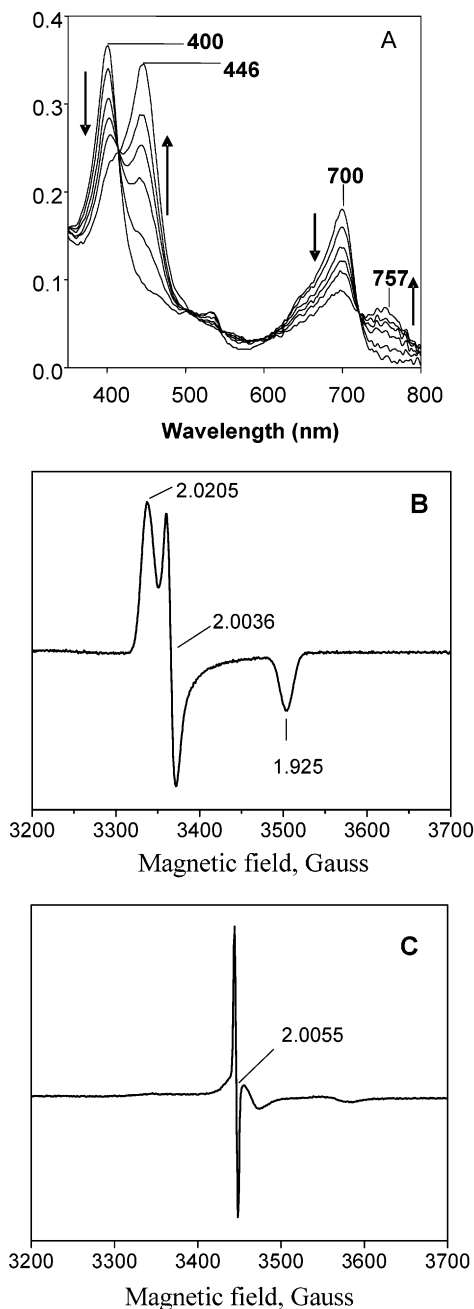


Figure 3. (A) Electronic absorption spectra obtained during the anaerobic reduction of the $[\text{Fe}^{\text{II}}(\text{verdoheme})]^+$ complex with sodium dithionite at pH 10 and EPR spectra corresponding to the product of reduction, acquired at (B) 90 K and at (C) ambient temperature, 295 K.

density residing in the macrocycle and by the relaxation properties of spin density residing in the metal. This is in agreement with the formulation of a resonance hybrid.

Resonance Raman spectra obtained with a 413 or 458 nm laser excitation within the Soret absorption of the reduced $[\text{Fe}^{\text{II}}(\text{verdoheme}\bullet)]$ complex at pH 10 display only very weak RR bands that correspond to those observed in the resting state $[\text{Fe}^{\text{II}}(\text{verdoheme}-b_5)]^+$ complex. The weak RR signals may originate from traces of unreduced material. Alternatively, the $[\text{Fe}^{\text{I}}(\text{verdoheme})]$ species could display vibrational frequencies comparable to those of the resting state complex if the reduction of the iron does not result in significant reorganization of the macrocycle structure. Whether these

(24) Donohoe, R. J.; Atamian, M.; Bocian, D. F. *J. Am. Chem. Soc.* **1987**, *109*, 5593–5599.

(25) Mashiko, T.; Reed, C. A.; Haller, K. J.; Scheidt, W. R. *Inorg. Chem.* **1984**, *23*, 3192–3196.

(26) Nahor, G. S.; Neta, P.; Hambright, P.; Robinson, L. R.; Harriman, A. *J. J. Phys. Chem.* **1990**, *94*, 6659–6663.

(27) Yamaguchi, K.; Morishima, I. *Inorg. Chem.* **1992**, *31*, 3216–3222.

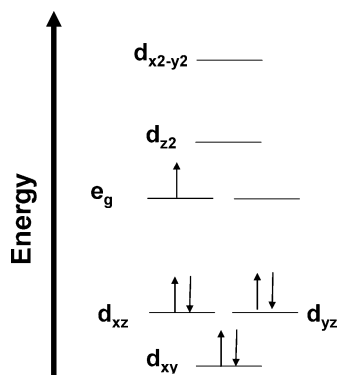


Figure 4. The electron-withdrawing oxygen atom in the $[\text{Fe}^{\text{II}}(\text{verdoheme})]^+$ complex is expected to lower the energy of the e_g macrocycle orbitals and axial coordination of the ferrous central ion by the histidine ligands in cyt b_5 expected to raise the energy of the iron d_{z^2} orbital. Consequently, one-electron reduction of the $[\text{Fe}^{\text{II}}(\text{verdoheme})]^+$ complex results in unpaired electron population of the verdoheme e_g orbitals.

signals come from the reduced material or traces of unreacted material, the experiments characterize $[\text{Fe}^{\text{II}}(\text{verdoheme}\bullet)]$ as a very poor resonance Raman scatterer. Although it remains largely unexplained, the same phenomenon is well documented with $[\text{FeTPP}]^-$ systems.^{24,28}

Ring reduction in $(\text{CN})_4\text{TPP}$ is thought to be a consequence of electron-withdrawing substituents on the porphyrin ring, which are thought to lower the energy of the porphyrin LUMO (e_g) orbitals.^{24,27,29} In the context of this work, the effect of the electron-withdrawing oxygen atom in the verdoheme macrocycle results in a similar lowering of the e_g orbitals, as is shown schematically in Figure 4. The axial histidine ligands in OM cytochrome b_5 are poised to coordinate to the central metal ion by virtue of the polypeptide fold.³⁰ Hence, it is not unreasonable that the reduced verdoheme center in cytochrome b_5 is axially coordinated, which results in destabilization of the d_{z^2} orbital. Consequently, reduction of $[\text{Fe}^{\text{II}}(\text{verdoheme})]^+$ results in the population of one of the e_g orbitals by an unpaired electron, which is consistent with the nearly isotropic $g \sim 2$ EPR signal (Figure 3C). The very small rhombic anisotropy seen in the EPR spectrum of $[\text{Fe}(\text{verdoheme}\bullet)]$ at 90 K (Figure 3B) may derive from symmetry-allowed interactions of the porphyrin e_g orbital and the iron d_{xz} and d_{yz} (d_{π}) orbitals, which is consistent with the formulation of $[\text{Fe}^{\text{II}}(\text{verdoheme}\bullet)] \leftrightarrow [\text{Fe}^{\text{I}}(\text{verdoheme})]$ resonance hybrids as an adequate representation of this species.

When a solution of ($[\text{Fe}^{\text{II}}(\text{verdoheme}\bullet)]$) is exposed to air the compound is readily and quantitatively reoxidized to the original verdoheme complex, $[\text{Fe}^{\text{II}}(\text{verdoheme})]^+$. This remarkable observation is in contrast to the previously reported oxidation of the bis(pyridine) Fe^{II} –verdoheme π -neutral radical, which in the presence of O_2 is converted into a species that exhibits an electronic absorption spectrum with a broad band near 778 nm.

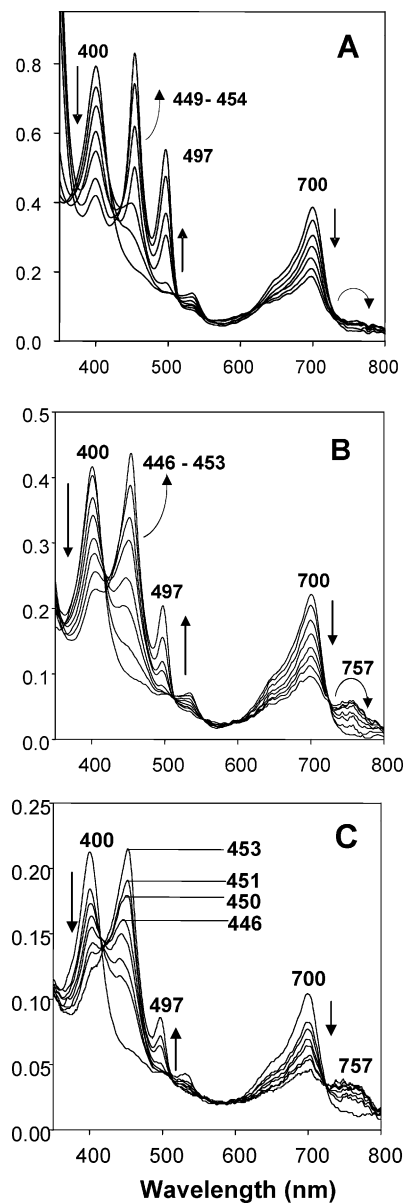


Figure 5. Electronic absorption spectra obtained during the anaerobic reduction of the $[\text{Fe}^{\text{II}}(\text{verdoheme})]^+$ complex with sodium dithionite at pH (A) 7.0, (B) 8.0, and (C) 9.0.

(b) Reduction of Fe^{II} – α -verdoheme b_5 at pH below 10.0. When sodium dithionite is added to an anaerobic solution of $[\text{Fe}^{\text{II}}(\text{verdoheme})]^+$ at pH 7.0, the band at 400 nm decreases slowly and is replaced by a split Soret with absorption maxima at 454 and 497 nm (Figure 5A). Note that the changes in electronic absorption spectra do not exhibit isosbestic points. This reduced species is EPR silent at ambient temperature, 77 K and 4 K. Close inspection of the electronic absorption spectra obtained as a function of time upon addition of excess dithionite to $[\text{Fe}^{\text{II}}(\text{verdoheme})]^+$ at pH 7.0 reveals that the most intense peak corresponding to the reduced species being formed displays a peak at 446 nm. As the reaction progresses, the intensity of this peak increases and shifts toward 454 nm with the simultaneous growth of a second peak (497 nm) corresponding to the split Soret. Among the two peaks in the split Soret, the peak at 497 nm does not shift as the reaction progresses. These

(28) De Silva, C.; Czarniecki, K.; Ryan, M. D. *Inorg. Chim. Acta* **1999**, 287, 21–26.

(29) Reed, C. A. *Adv. Chem. Ser.* **1982**, 333–356.

(30) Rodriguez-Maranon, M. J.; Feng, Q.; Stark, R. E.; White, S. P.; Zhang, X.; Foundling, S. I.; Rodriguez, V.; Schilling, C. L., III; Bunce, R. A.; Rivera, M. *Biochemistry* **1996**, 35, 16378–16390.

observations suggest that at pH 7.0 $[\text{Fe}^{\text{II}}(\text{verdoheme})]^+$ is initially reduced to the same α -verdoheme b_5 π -neutral radical complex ($[\text{Fe}^{\text{II}}(\text{verdoheme}\bullet)]$) that is observed upon reduction at pH 10, which exhibits a Soret peak at 446 nm (see Figure 3). However, at pH 7.0 this complex reacts further to give an EPR-inactive species exhibiting a split Soret at 454 and 497 nm. Consistent with the initial accumulation of $[\text{Fe}^{\text{II}}(\text{verdoheme}\bullet)]$ there is an initial increase in intensity of the band at 757 nm, which is followed by a decrease in its intensity as the peak at 446 nm grows and shifts toward 454 nm and the second peak in the split Soret band (497 nm) becomes more intense. Similar observations were made at pH 8.0 (Figure 5B). As with the species obtained at pH 7, the complex formed at pH 8.0 is EPR silent and displays the same split Soret absorption.

When excess dithionite is added at pH 9.0, the peak at 400 nm decreases with the concomitant appearance and growth of a peak at 446 nm (Figure 5C); the latter corresponds to the Soret band of the $[\text{Fe}^{\text{II}}(\text{verdoheme}\bullet)]$, which is EPR active (see Figure 3). It is interesting, however, that later in the reaction the peak at 446 nm shifts toward 453 nm and a peak at 497 nm appears and grows. These observations suggest that $[\text{Fe}^{\text{II}}(\text{verdoheme}\bullet)]$ accumulates to a significant extent at pH 9.0 before it is converted to an EPR silent species displaying the split Soret band. On the other hand, at pH 10, $[\text{Fe}^{\text{II}}(\text{verdoheme}\bullet)]$ can be obtained pure or with limited conversion to the species displaying the split Soret band (vide supra). As was observed with the reduced species obtained at pH 10, exposure of the reduced species generated at pH 7.0, 8.0, or 9.0 to O_2 results in their quantitative conversion to the original $[\text{Fe}^{\text{II}}(\text{verdoheme})]^+$ complex.

It is likely that the species exhibiting a split Soret band and no EPR spectrum is obtained from a two-electron reduction of $[\text{Fe}^{\text{II}}(\text{verdoheme})]^+$. An EPR-silent species is also obtained upon two-electron reduction of $\text{Fe}^{\text{II}}\text{TPP}$;²⁹ this two-electron reduced species is thought to exist as a resonance hybrid,^{25,29} $[\text{Fe}^{\text{I}}(\text{TPP}\bullet)]^{2-} \leftrightarrow [\text{Fe}^{\text{II}}(\text{TPP:})]^{2-}$. It is thus possible that the two-electron-reduced $[\text{Fe}^{\text{II}}(\text{verdoheme})]^+$, hereafter termed α -verdoheme- b_5 anion, $[\text{Fe}^{\text{II}}(\text{verdoheme:})]^-$, may exist as a resonance hybrid, $[\text{Fe}^{\text{I}}(\text{verdoheme}\bullet)]^- \leftrightarrow [\text{Fe}^{\text{II}}(\text{verdoheme:})]^-$. However, at present it is not possible to eliminate the possibility that the two-electron-reduced species possesses iron in the Fe(0) oxidation state or if an Fe(0) species contributes to the resonance hybrid. When this species was studied by RR spectroscopy using 458 nm excitation (Figure 6B), strong resonance enhanced bands were observed in the 1200–1650 cm^{-1} range. In the mid-frequency range, the bands at 1260, 1361, and 1437 cm^{-1} are reminiscent of those detected in the resting state Fe^{II} verdoheme complex (Figure 6A) but clearly different. In the high-frequency region, a broad feature composed of at least three modes is centered at ~ 1622 cm^{-1} . These intense spectral features are in contrast to the near RR-silent character of the one-electron-reduced species formed at pH 10 and therefore support the notion of a two-electron-reduced macrocycle with skeletal modes clearly distinct from those of the resting $[\text{Fe}^{\text{II}}(\text{verdoheme})]^+$ complex. Additional work

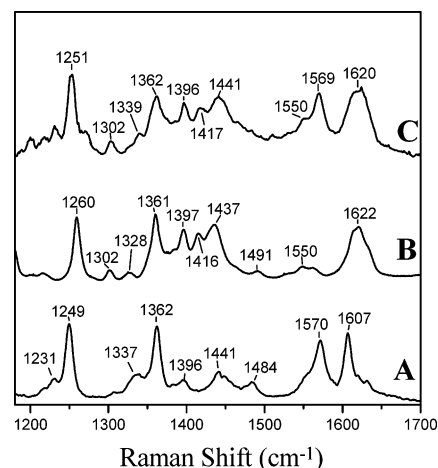


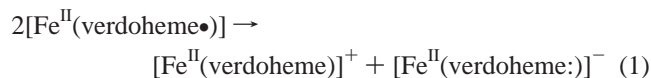
Figure 6. Resonance Raman spectra (458 nm excitation) of (A) the $[\text{Fe}^{\text{II}}(\text{verdoheme})]^+$ complex and the reduced species formed at (B) pH 7.0 and (C) pH 10.0. All the observed features can be accounted for by residual contributions from the resting state $[\text{Fe}^{\text{II}}(\text{verdoheme})]^+$ complex and the split Soret $[\text{Fe}^{\text{II}}(\text{verdoheme:})]^-$ species.

will be required to utilize these RR spectra to their full potential. Attempts were also made to study the nature of the one- and two-electron-reduced verdoheme complexes by ^1H NMR spectroscopy. However, peaks resolved from the intense envelope of diamagnetic resonances originating from the polypeptide were not observed, despite the fact that these signals were searched with the typically large spectral widths and fast repetition cycles necessary to detect paramagnetically affected resonances.³¹

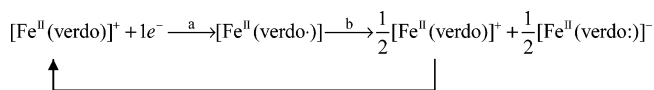
The observations presented above indicate that at the lower pH values (7.0 and 8.0) small amounts of the one-electron-reduced $[\text{Fe}^{\text{II}}(\text{verdoheme}\bullet)]$ complex accumulate in the initial stages of the reaction with excess (5–10 equiv) dithionite. However, as the reaction progresses, the small amounts of accumulated $[\text{Fe}^{\text{II}}(\text{verdoheme}\bullet)]$ convert to the two-electron-reduced $[\text{Fe}^{\text{II}}(\text{verdoheme:})]^-$ complex. Indeed, at pH 7.0 and 8.0, addition of dithionite results in almost quantitative formation of the two-electron-reduced complex. In contrast, when the reduction of $[\text{Fe}^{\text{II}}(\text{verdoheme})]^+$ is carried out at pH 10, accumulation of the one-electron-reduced $[\text{Fe}^{\text{II}}(\text{verdoheme}\bullet)]$ complex is nearly quantitative. Although these observations seem to indicate that $[\text{Fe}^{\text{II}}(\text{verdoheme}\bullet)]$ is further reduced by dithionite to $[\text{Fe}^{\text{II}}(\text{verdoheme:})]^-$ at pH 7.0 and 8.0, it is important to consider that the reduction potential of dithionite is more positive at pH 7.0 ($E^{\circ'} = -0.532$ V vs NHE) than at pH 10.0 ($E^{\circ'} = -0.767$ V).³² Thus, while the formation of $[\text{Fe}^{\text{II}}(\text{verdoheme:})]^-$ is nearly quantitative at pH 7.0 and 8.0, a negligible amount of this species is formed at pH 10 despite the increased reducing power of dithionite at higher pH. Consequently, we favor an alternative route for the formation of the two-electron-reduced $[\text{Fe}^{\text{II}}(\text{verdoheme:})]^-$ complex, namely, the disproportionation of the $[\text{Fe}^{\text{II}}(\text{verdoheme}\bullet)]$ complex, as shown in eq 1.

(31) La Mar, G. N.; Satterlee, J. D.; De Ropp, J. S. In *The Porphyrin Handbook*, 5, Nuclear Magnetic Resonance of Hemoproteins; Kadish, K. M., Smith, K. M., Guilard, R., Eds.; Academic Press: New York, 2000; pp 185–297.

(32) Mayhew, S. G. *Eur. J. Biochem.* **1978**, *85*, 535–547.



The disproportionation reaction appears to be more efficient at lower pH because addition of excess dithionite in the absence of O_2 results in very little accumulation of the π -neutral radical at pH 7.0 and 8.0, whereas at pH 9.0 this species has a relatively low tendency to disproportionate and at pH 10.0 it is stable for at least 30 min. Indeed, when $[\text{Fe}^{\text{II}}(\text{verdoheme}\bullet)]$ is prepared at pH 10.0 by addition of 5 equiv of dithionite to a solution of $[\text{Fe}^{\text{II}}(\text{verdoheme})]^+$ in a glovebox, the product displays the characteristic electronic absorption spectrum of $[\text{Fe}^{\text{II}}(\text{verdoheme}\bullet)]$ with a single Soret peak at 446 nm (red in Figure 7A). When the pH of this solution was lowered to 7.0 by addition of nitric acid, while the solution was maintained as anaerobic, the electronic absorption spectrum of the resultant solution reveals a near 1:1 mixture of resting state $[\text{Fe}^{\text{II}}(\text{verdoheme})]^+$ and two-electron-reduced $[\text{Fe}^{\text{II}}(\text{verdoheme:})]^-$ species (green in Figure 7A). These observations clearly indicate that as the pH is changed from 10.0 to 7.0, the π -neutral radical species, which is stable at pH 10.0, readily disproportionates according to eq 1. Hence, near quantitative formation of $[\text{Fe}^{\text{II}}(\text{verdoheme:})]^-$ at the lower pH values is likely produced by the set of reactions summarized below, where the resting state $[\text{Fe}^{\text{II}}(\text{verdoheme})]^+$ complex produced by disproportionation is reduced by excess dithionite to $[\text{Fe}^{\text{II}}(\text{verdoheme}\bullet)]$. The latter disproportionates upon encountering a second $[\text{Fe}^{\text{II}}(\text{verdoheme}\bullet)]$ molecule and continues the cycle that results in nearly quantitative formation of the two-electron-reduced $[\text{Fe}^{\text{II}}(\text{verdoheme:})]^-$ anion.



- a) dithionite reduction: slow at pH 7, fast at pH 10
b) disproportionation: fast at pH 7, slow at pH 10

At pH 9.0 the disproportionation reaction is less favorable, thus permitting significant accumulation of the $[\text{Fe}^{\text{II}}(\text{verdoheme}\bullet)]$ radical. At pH 10.0 the disproportionation reaction is very slow and the $[\text{Fe}^{\text{II}}(\text{verdoheme}\bullet)]$ radical can fully accumulate before the characteristic split Soret peaks of the two-electron-reduced species start to appear after several hours at room temperature.

The disproportionation of the $[\text{Fe}^{\text{II}}(\text{verdoheme}\bullet)]$ complex occurs at all pH values. However, the rate of disproportionation is relatively fast at pH 7.0 and becomes progressively slower as the pH increases; at pH 10 the disproportionation reaction occurs very slowly but proceeds to completion in approximately 36 h. This indicates that pH influences the rate of disproportionation but does not have a pronounced effect on the stability of the $[\text{Fe}^{\text{II}}(\text{verdoheme}\bullet)]$ complex relative to those corresponding to the resting state $[\text{Fe}^{\text{II}}(\text{verdoheme})]^+$ and two-electron-reduced $[\text{Fe}^{\text{II}}(\text{verdoheme:})]^-$ species. This behavior is perhaps best explained in the context of Figure 8, which shows the electrostatic surface of mitochondrial cytochrome b_5 ,³⁰ where negative electrostatic

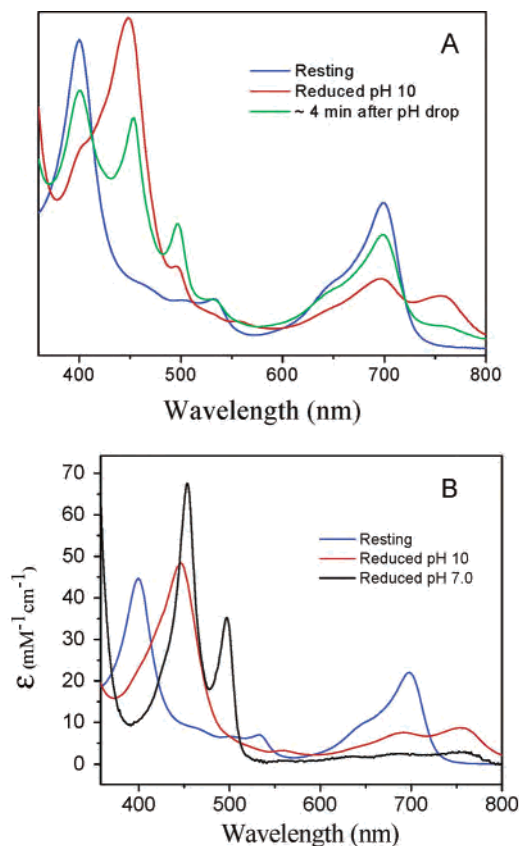


Figure 7. (A) $[\text{Fe}^{\text{II}}(\text{verdoheme})]^+$ complex equilibrated with pH 10 buffer (blue) and reduced with excess dithionite to the one-electron-reduced $[\text{Fe}^{\text{II}}(\text{verdoheme}\bullet)]^+$ complex (red). Lowering the pH to 7.0 results in the formation of a mixture of resting state $[\text{Fe}^{\text{II}}(\text{verdoheme})]^+$ split Soret $[\text{Fe}^{\text{II}}(\text{verdoheme:})]^-$ (green). (B) Spectra corresponding to $[\text{Fe}^{\text{II}}(\text{verdoheme})]^+$ (blue), $[\text{Fe}^{\text{II}}(\text{verdoheme}\bullet)]^+$ (red), and $[\text{Fe}^{\text{II}}(\text{verdoheme:})]^-$ (black) shown for reference.

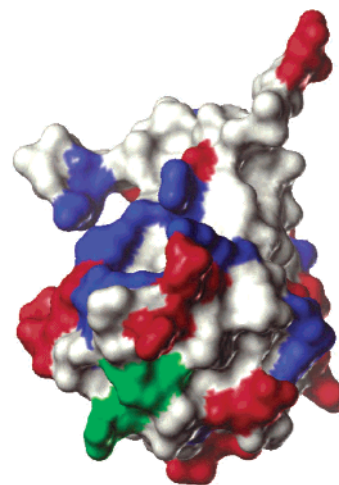


Figure 8. View of the surface electrostatic potential corresponding to rat OM cytochrome b_5 (PDB 1B5M). Red represents negative electrostatic potential, blue represents positive electrostatic potential, and gray is neutral. The heme is shown in green to facilitate its visualization. The heme propionates contribute to the negative surface electrostatic potential of rat OM b_5 .

surfaces are shown in red, positive electrostatic surfaces are in blue and neutral in gray. The heme has been colored green to facilitate its visualization, but it should be remembered that the heme (verdoheme) propionates contribute to the

negative surface electrostatic potential of cytochrome b_5 . At pH 7.0 the surface of cytochrome b_5 exhibits localized surfaces with positive and negative electrostatic potential near the heme. It is thus reasonable to expect transient complex formation between two $[\text{Fe}^{\text{II}}(\text{verdoheme}\bullet)]$ -containing cytochrome b_5 molecules via docking of opposite electrostatic potential surfaces. The resulting proximity between the active sites of the two proteins in the complex can promote electron transfer, i.e., the disproportionation reaction between two $[\text{Fe}^{\text{II}}(\text{verdoheme}\bullet)]$ molecules. In contrast, at pH 10, the positive surface electrostatic potential decreases as Lys and Arg residues begin to be neutralized (Figure 8). However, as negative surface electrostatic potential remains unchanged, electrostatic repulsion between negatively charged $[\text{Fe}^{\text{II}}(\text{verdoheme}\bullet)]$ molecules interferes with the formation of a complex and thus significantly decreases the rate of electron transfer that leads to disproportionation. This notion is not only in agreement with the experimental observations described here, but it also finds support in the fact that changes in the surface electrostatic potential of cytochrome b_5 result in changes in rate constants of electron self-exchange.^{33,34}

Discussion

Reports of previous studies conducted with Fe^{II} -verdoheme complexes of myoglobin⁷ and pyridine^{10,11} propose that the oxidation of verdoheme to biliverdin is initiated with a one-electron reduction of Fe^{II} -verdoheme to form a verdoheme π -neutral radical, as shown in Scheme 2. More recently, it was shown¹⁸ that addition of dithionite to an anaerobic solution of the Fe^{II} -verdoheme complex of heme oxygenase results in the formation of a species exhibiting an electronic absorption spectrum very similar to those of the bis(pyridine)¹⁰ and cytochrome b_5 (pH 10; Figure 3) complexes of the Fe^{II} -verdoheme π -neutral radical. In this context, it is interesting that addition of NADPH and cytochrome P-450 reductase to an anaerobic solution of the Fe^{II} -verdoheme complex of heme oxygenase did not affect the electronic absorption spectrum of the latter.¹⁸ This observation strongly suggests that ring reduction of verdoheme is not a path followed by heme oxygenase under physiological conditions. On the other hand, observations indicating that Zn^{II} - and Fe^{II} -verdoheme π -neutral radical complexes of pyridine^{10,11} and myoglobin⁹ decay to a species exhibiting a spectrum resembling that of biliverdin upon

exposure to air suggest that an alternative path may be operative in vitro. In fact, in recent years it has become evident that the mechanism of heme hydroxylation in heme oxygenase is different from that followed by the coupled oxidation reaction.^{35–37}

The observations made during our studies with the Fe^{II} -verdoheme complex of cytochrome b_5 ($[\text{Fe}^{\text{II}}(\text{verdoheme})]^+$) are in agreement with the relative predisposition of the Fe^{II} -verdoheme ring to be reduced.^{5,10} This propensity likely originates from the presence of an electron-withdrawing oxygen atom within the verdoheme macrocycle (vide supra). Contrary to expectations, however, exposure of the singly reduced $[\text{Fe}^{\text{II}}(\text{verdoheme}\bullet)]$ or doubly reduced $[\text{Fe}^{\text{II}}(\text{verdoheme})]^-$ complexes of cyt b_5 to air resulted in rapid and quantitative oxidation to the parent $[\text{Fe}^{\text{II}}(\text{verdoheme})]^+$ complex. This remarkable observation adds to the repertoire of reactions documented for verdoheme, which encompasses changes in oxidation state, axial coordination state, and spin state, while maintaining the structural integrity of the macrocycle.^{4,6} It is interesting to contrast the O_2 oxidation of the verdoheme π -neutral radical complex of cytochrome b_5 with the oxidation reported for the bis(pyridine) and myoglobin complexes of Zn^{II} - and Fe^{II} -verdoheme π -neutral radicals. When these complexes are exposed to O_2 , the verdoheme π -neutral radical is converted into a species exhibiting an absorption spectrum similar to that of biliverdin.^{9–11} The contrasting behavior of the verdoheme π -neutral radical in cytochrome b_5 is likely to be related to the accessibility of the α -meso ring position. If the verdoheme macrocycle binds to cytochrome b_5 as heme does, the oxygen atom of the α -verdoheme ring will be buried at the bottom of the binding pocket. Steric constraints would prevent the efficient diffusion of O_2 to the pyrrole- α carbons adjacent to the oxygen atom in the verdoheme ring, thus preventing its reaction with the porphyrin radical (see reaction 5 in Scheme 2). Instead, because the unpaired electron in the verdoheme π -neutral radical $[\text{Fe}^{\text{II}}(\text{verdoheme}\bullet)]$ possesses some degree of metal character, oxidation of verdoheme within the binding pocket of cytochrome b_5 can occur via outer-sphere oxidation of the metal center.

Acknowledgment. This work was supported by NIH Grants GM-50503 (M.R.) and GM-18865 (P.M.-L.)

IC049029K

(33) Ma, D.; Wu, Y.; Qian, C.; Tang, W.; Wang, Y.-H.; Wang, W.-H.; Lu, J.-X.; Xie, Y.; Huang, Z.-X. *Inorg. Chem.* **1999**, *38*, 5749–5754.
 (34) Dixon, D. W.; Hong, X.; Woehler, S. E.; Mauk, A. G.; Sishta, B. P. *J. Am. Chem. Soc.* **1990**, *112*, 1082–1088.

(35) Sigman, J. A.; Wang, X.; Lu, Y. *J. Am. Chem. Soc.* **2001**, *123*, 6945–6946.

(36) Avila, L.; Huang, H.; Damaso, C. O.; Lu, S.; Moënne-Loccoz, P.; Rivera, M. *J. Am. Chem. Soc.* **2003**, *125*, 4103–4110.

(37) St. Claire, T. N.; Balch, A. L. *Inorg. Chem.* **1999**, *38*, 684–691.